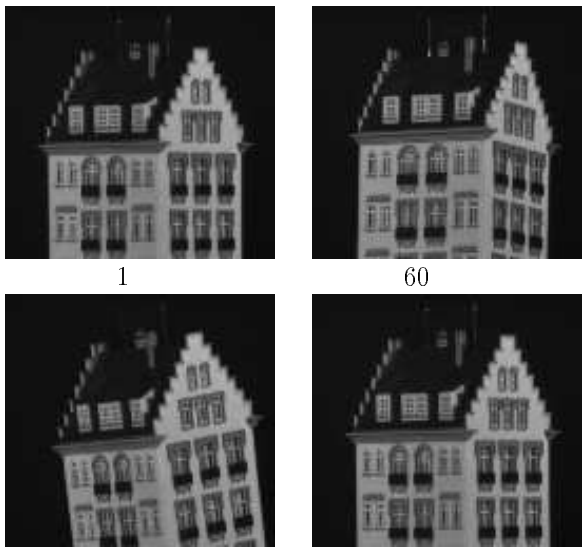

Figure 4.1: Some frames in the sequence. The whole sequence is 150 frames.

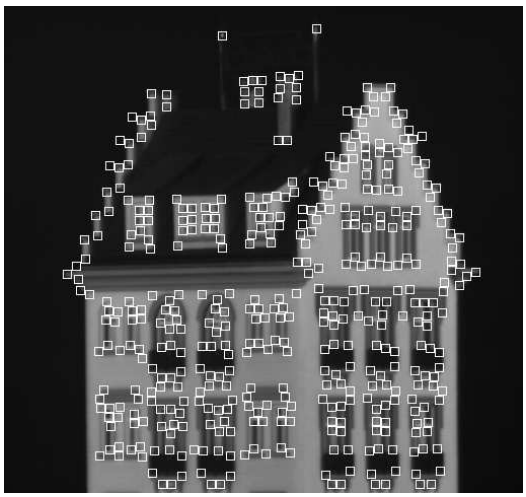

Figure 4.3: The 430 features selected by the automatic detection method.

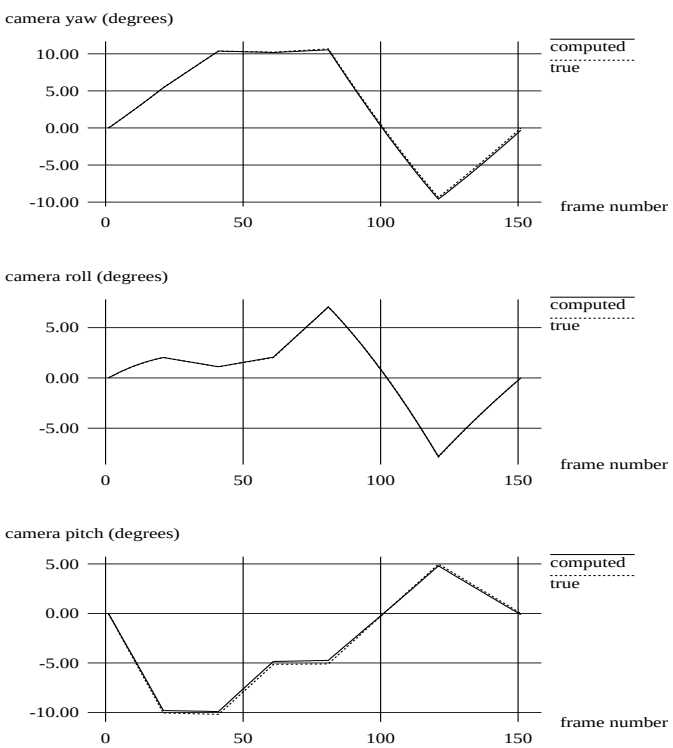

Figure 4.2: True and computed camera yaw, roll, pitch.

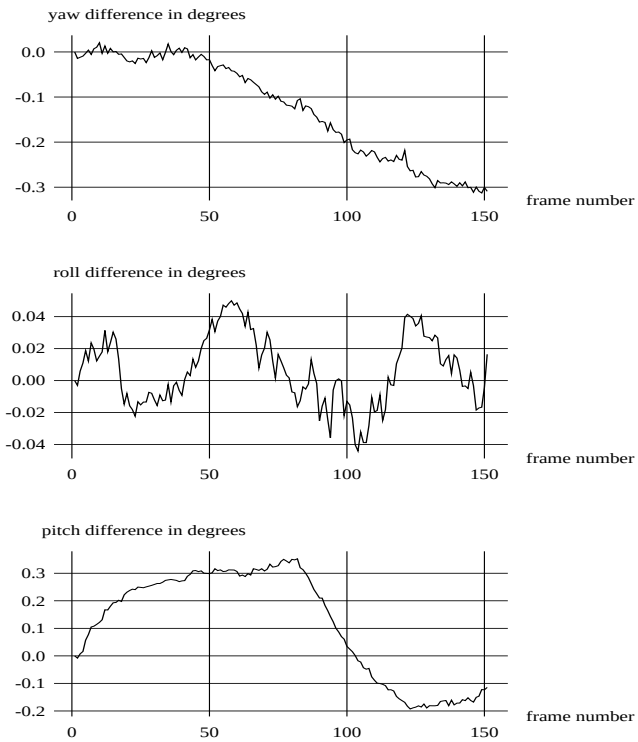

Figure 4.4: Blow-up of the errors in figure 4.2.

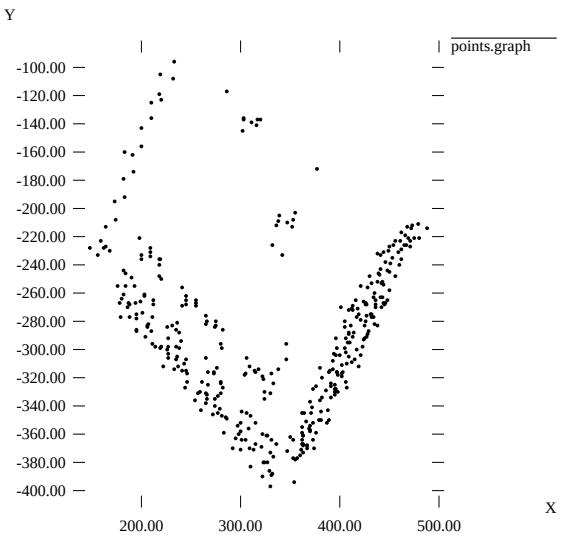

Figure 4.5: A view of the computed shape from approximately above the building (compare with figure 4.6).

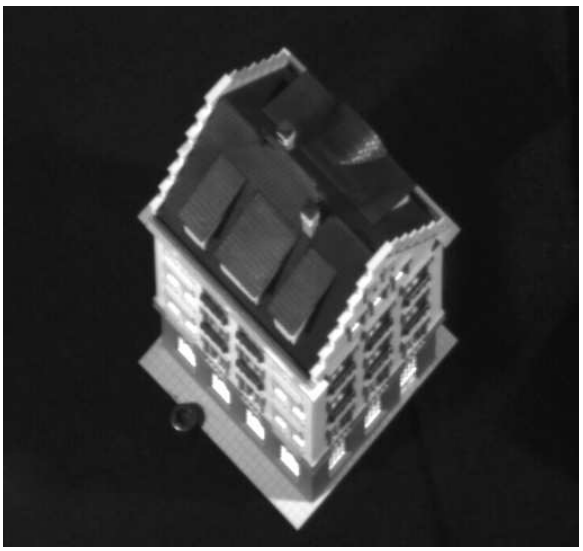

Figure 4.6: A real picture from above the building, similar to figure 4.5.

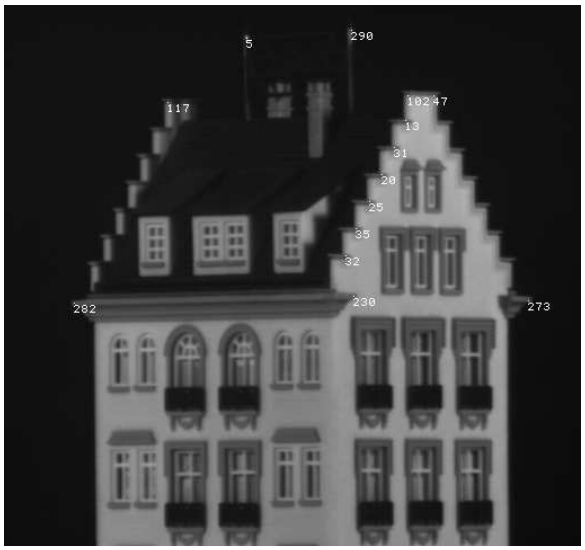

Figure 4.7: For a quantitative evaluation, distances between the features shown in the picture were measured on the actual model, and compared with the computed results. The comparison is shown in figure 4.8.

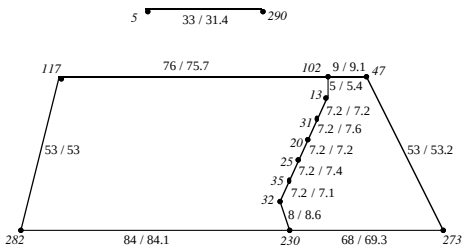

Figure 4.8: Comparison between measured and computed distances for the features in figure 4.7. The number before the slash is the measured distance, the one after is the computed distance. Lengths are in millimeters. Computed distances were scaled so that the computed distance between features 117 and 282 is the same as the measured distance.

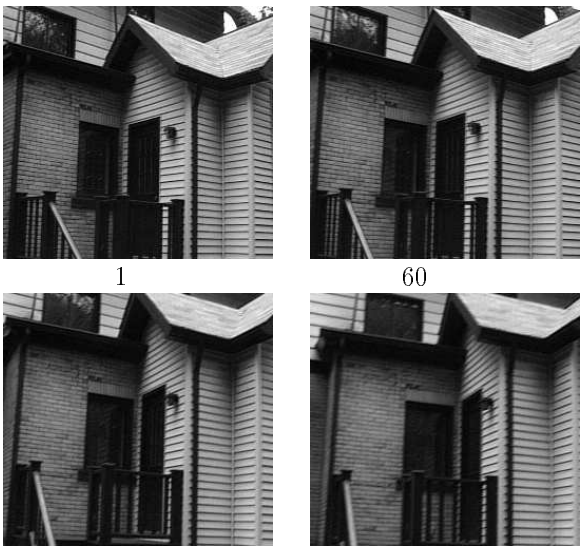

Figure 4.9: Four out of the 180 frames of the real house image stream.

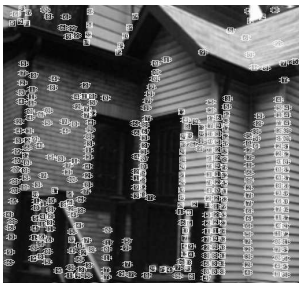

Figure 4.10: The features selected in the first frame of the real house stream (figure 4.9)
.

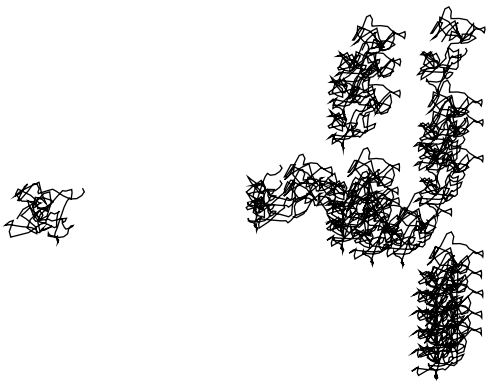

Figure 4.11: Tracks of 60 randomly selected features from the real house stream (figure 4.9.)

Figure 4.12: A front view of the three reconstructed walls, with the original image intensities mapped onto the resulting surface.

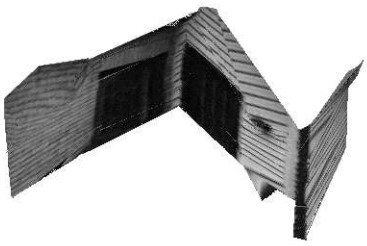

Figure 4.13: A view from above of the three reconstructed walls, with image intensities mapped onto the surface.

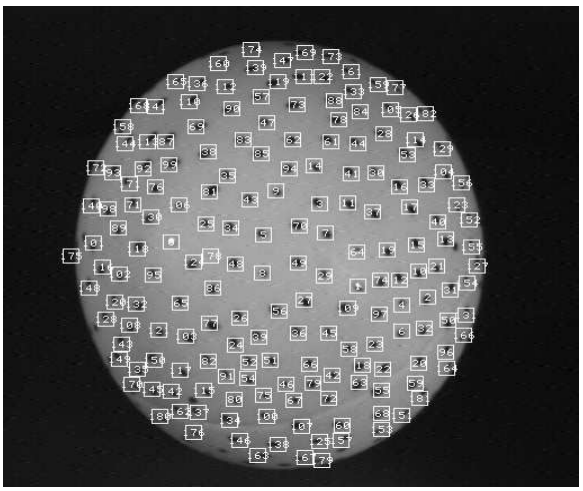

Figure 6.14: The first frame of the ping-pong stream, with overlaid features.

Figure 6.15: Tracks of 60 randomly selected features from the stream of figure 6.14.

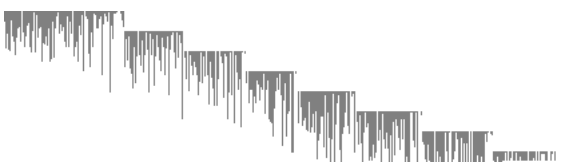

Figure 6.16: The fill matrix for the ping-pong ball experiment. Shaded entries are known.

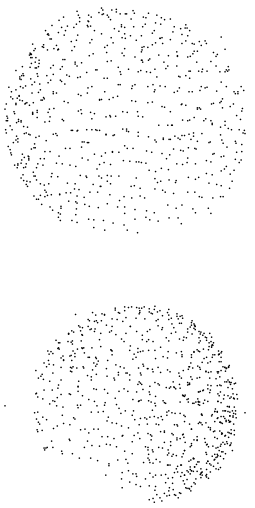

Figure 6.17: Top and side views of the reconstructed ping-pong ball.

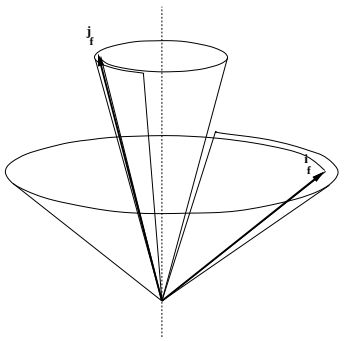

Figure 6.18: Rotational component of the camera motion for the ping-pong stream. Because rotation occurs around a fixed axis, the two mutually orthogonal unit vectors $\mathbf{i}_f$ and $\mathbf{j}_f$, pointing along rows and columns of the image sensor, sweep two 450-degree cones in space.

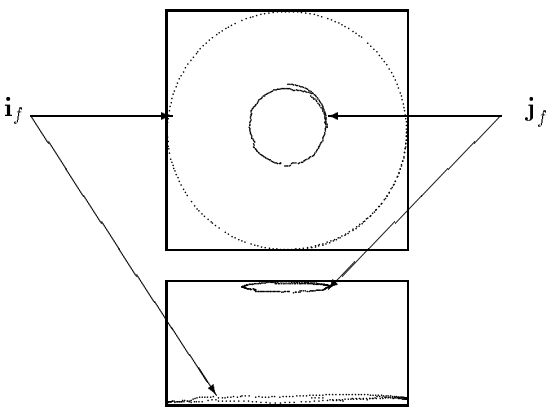

Figure 6.19: Top and side views of the $\mathbf{i}_f$ and $\mathbf{j}_f$ vectors identifying the camera rotation. See Figure 6.18.

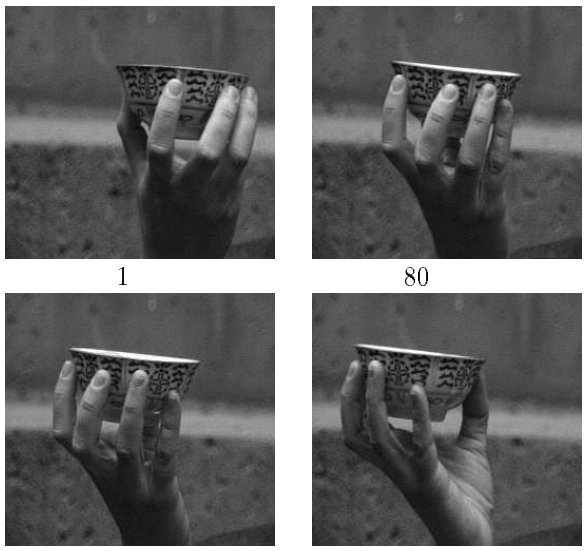

Figure 6.20: Four out of the 240 frames of the cup image stream.

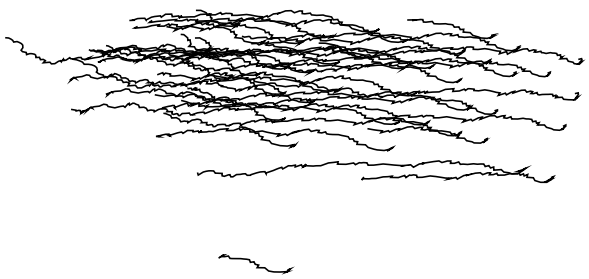

Figure 6.21: Tracks of 60 randomly selected features from the cup stream.

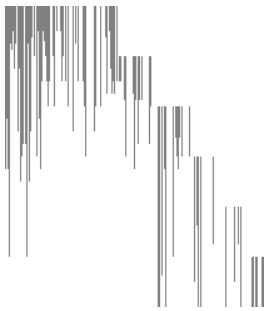

Figure 6.22: The 240×207 fill matrix for the cup stream (figure 6.20). Shaded entries are known.

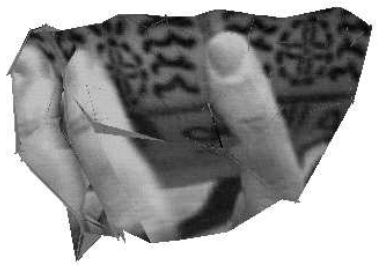

Figure 6.23: A front view of the cup and fingers, with the original image intensities mapped onto the resulting surface.

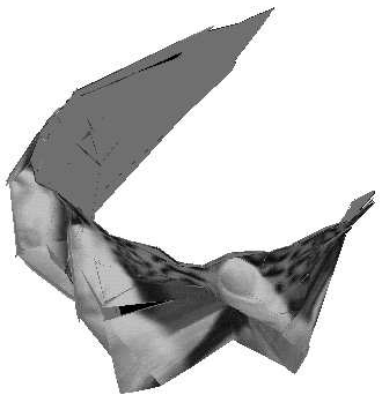

Figure 6.24: A view from above of the cup and fingers with image intensities mapped onto the surface.